PLOS ONE

RESEARCH ARTICLE

Response of Spring Diatoms to CO_2 Availability in the Western North Pacific as Determined by Next-Generation Sequencing

Hisashi Endo[1,2]*, Koji Sugie[3,4☯], Takeshi Yoshimura[3☯], Koji Suzuki[1,2☯]

1 Faculty of Environmental Earth Science/Graduate School of Environmental Science, Hokkaido University, Sapporo, Hokkaido, Japan, **2** CREST, Japan Science and Technology, Sapporo, Hokkaido, Japan, **3** Central Research Institute of Electric Power Industry, Abiko, Chiba, Japan, **4** Research and Development Center for Global Change, Japan Agency for Marine Earth-Science and Technology (JAMSTEC), Yokosuka, Kanagawa, Japan

☯ These authors contributed equally to this work.
* endo@ees.hokudai.ac.jp

Citation: Endo H, Sugie K, Yoshimura T, Suzuki K (2016) Response of Spring Diatoms to CO_2 Availability in the Western North Pacific as Determined by Next-Generation Sequencing. PLoS ONE 11(4): e0154291. doi:10.1371/journal.pone.0154291

Editor: Amanda M Cockshutt, Mount Allison University, CANADA

Received: November 25, 2015

Accepted: April 12, 2016

Published: April 28, 2016

Data Availability Statement: All relevant data are within the paper and its Supporting Information files. All sequencing files are available from the DDBJ Sequence Read Archive (DRA) database (accession number DRA003722).

Funding: This work was supported by grants from the Central Research Institute of Electric Power Industry (No. 090313; URL: http://criepi.denken.or.jp/en/) and Grants-in-Aid for Scientific Research (No. 18067008, 22681004, and 24121004; URL: https://www.jsps.go.jp/english/e-grants/). The funders had

Abstract

Next-generation sequencing (NGS) technologies have enabled us to determine phytoplankton community compositions at high resolution. However, few studies have adopted this approach to assess the responses of natural phytoplankton communities to environmental change. Here, we report the impact of different CO_2 levels on spring diatoms in the Oyashio region of the western North Pacific as estimated by NGS of the diatom-specific *rbcL* gene (DNA), which encodes the large subunit of RubisCO. We also examined the abundance and composition of *rbcL* transcripts (cDNA) in diatoms to assess their physiological responses to changing CO_2 levels. A short-term (3-day) incubation experiment was carried out on-deck using surface Oyashio waters under different pCO_2 levels (180, 350, 750, and 1000 μatm) in May 2011. During the incubation, the transcript abundance of the diatom-specific *rbcL* gene decreased with an increase in seawater pCO_2 levels. These results suggest that CO_2 fixation capacity of diatoms decreased rapidly under elevated CO_2 levels. In the high CO_2 treatments (750 and 1000 μatm), diversity of diatom-specific *rbcL* gene and its transcripts decreased relative to the control treatment (350 μatm), as well as contributions of Chaetocerataceae, Thalassiosiraceae, and Fragilariaceae to the total population, but the contributions of Bacillariaceae increased. In the low CO_2 treatment, contributions of Bacillariaceae also increased together with other eukaryotes. These suggest that changes in CO_2 levels can alter the community composition of spring diatoms in the Oyashio region. Overall, the NGS technology provided us a deeper understanding of the response of diatoms to changes in CO_2 levels in terms of their community composition, diversity, and photosynthetic physiology.

no role in study design, data collection and analysis, decision to publish, or preparation of the manuscript.

Competing Interests: The authors have declared that no competing interests exist.

Introduction

Progressive increases in the seawater partial pressure of CO_2 (pCO_2) and decreases in pH (i.e., ocean acidification, [1]) caused by industrial CO_2 emissions could affect biological processes in the ocean [2]. Because CO_2 is the primary substrate for photosynthesis, ocean acidification can enhance CO_2 availability for marine phytoplankton. Accordingly, ocean acidification could play key roles in controlling productivity and organic matter production [3–5], thereby potentially affecting the biogeochemical and ecological processes in the ocean.

Studies on the impacts of increased CO_2 levels have been conducted on a variety of phytoplankton species [3, 6, 7, 8]. In the context of the global carbon cycle and feedbacks to climate change, diatoms are an important class of phytoplankton because they are responsible for approximately 40% of total primary production in the global ocean [9]. Comparative studies suggested that the growth of diatoms tended to increase with elevated CO_2 levels [10, 11]. Indeed, previous field studies have provided some evidence that elevated CO_2 levels could enhance the growth of diatoms in the Equatorial Pacific [12], the North Atlantic [13], and the Southern Ocean [14]. However, no significant or negative effects of elevated CO_2 on diatoms have been reported from the bloom-inducing field incubation experiments in the Raunefjord [15], the Western Subarctic Gyre (WSG) of the North Pacific [16], and the Bering Sea basin [17, 18]. These discrepancies could be caused by the species-specific differences in CO_2 response [19], although experimental conditions and other environmental factors might also affect the outcomes. Hence, detailed taxonomic information on diatoms would be indispensable for understanding their responses to changes in CO_2 levels in seawater.

In addition, marine diatoms can experience a decrease in CO_2 availability in some oceanic regions. In the Oyashio region of the western North Pacific, the pCO_2 in surface seawater decrease significantly from winter (ca. 400 μatm) to spring (< 200 μatm) as a consequence of intense diatom blooms [20]. Previous studies have suggested that diatoms can overcome low CO_2 availability by using biophysical CO_2-concentrating mechanisms (CCMs), which provide a high CO_2 concentration at the site of carboxylation [21, 22]. However, some experiments demonstrated that the growth and productivity of diatoms decreased under low CO_2 (100–220 μatm) conditions [7, 23]. At present, it is largely unknown how diatom assemblages respond to decrease in CO_2 availability, which occurs during spring blooms in the Oyashio region.

Recently, molecular biological techniques have become important tools for understanding the community composition and biodiversity of natural microbial assemblages including phytoplankton based on DNA sequence information [24–26]. It is reported that the abundance of particular genes can be an indicator of phytoplankton pigment biomass [27]. These techniques can also be applied to assess the responses of phytoplankton assemblages under different CO_2 levels [28–30]. For example, Hopkinson et al. [28] used 18S rRNA and nitrate reductase (NR) gene fragments to estimate the community compositions of haptophytes and diatoms, respectively, in different CO_2 levels. In addition, the *rbcL* gene, which encodes the large subunit of the enzyme ribulose bisphosphate carboxylase/oxygenase (RubisCO), was also used to estimate the abundance and community composition of phytoplankton assemblages during the CO_2-controlled mesocosm experiment conducted off the Norwegian coast [29]. These authors demonstrated a rapid shift in the community composition of pico-sized prasinophytes (i.e. *Bathycoccus* and *Micromonas*), which were difficult to identify by light microscopy, in response to increased CO_2 levels.

In addition, mRNA (cDNA) transcripts of functional genes could be a proxy for physiological responses of phytoplankton assemblages to environmental change. For example, the transcript levels of the *rbcL* gene could be an indicator of productivity because CO_2 is assimilated

via RubisCO in the Calvin-Benson-Bassham (CBB) cycle [31, 32]. Changes in gene expression and protein synthesis levels of RubisCO occur within a few hours in response to environmental change such as light and nutrient availability [33–35]. Therefore, it can be used to infer the potential effect of different CO_2 levels on the natural phytoplankton assemblages even from short-term incubation experiment. Endo et al. [27] showed that diatom-specific *rbcL* transcripts decreased in response to elevated CO_2 levels after 2 or 3 days of incubation in the Bering Sea. They also showed that a shift occurred in the community composition of photosynthetically active diatoms with an increase in seawater CO_2 levels. However, the conventional molecular cloning method with Sanger sequencing [36], which was used in previous studies, is sometimes inadequate for the extraction of comprehensive information from environmental samples, due to limited throughput, and may therefore underestimate the taxonomic richness of microbial assemblages [37, 38].

Recent advances in next-generation sequencing (NGS) technologies can overcome this limitation because these deep sequencing technologies can now generate several hundred thousand reads per sample [39]. Practically, metagenomic and amplicon sequencing using NGS platforms have been used to reveal the community composition and/or diversity of bacteria [40], phytoplankton [41], and zooplankton [42] in marine environments. However, to the best of our knowledge, these new technologies have not been used to estimate the effects of CO_2 availability on marine phytoplankton assemblages.

Here, we report the use of NGS technologies in combination with real-time PCR (qPCR) and HPLC pigment analysis to improve our understanding of the effects of CO_2 availability on the community structure and photosynthetic physiology of diatoms in the Oyashio region. Because of the massive diatom blooms in spring, this region has one of the greatest capacities for seasonal biological drawdown of pCO_2 in surface waters among the world's oceans [43]. Field observations revealed that the blooms were mainly composed of centric diatoms, such as *Chaetoceros* spp. and *Thalassiosira* spp. [44–47]. Taniguchi [48] noted that these diatoms contribute to the efficient energy transfer to higher trophic levels in the Oyashio region from spring to summer. Consequently, the spring diatom blooms significantly contribute to the formation of the highly productive fishing grounds in Oyashio and its surrounding waters [48, 49]. However, despite the crucial roles of diatom blooms in the ecosystems and biogeochemical processes, there are no reports on the impacts of different CO_2 availability on phytoplankton assemblages in the Oyashio region. We therefore conducted an on-deck incubation experiment using spring Oyashio waters under different pCO_2 levels.

Materials and Methods

Seawater samples used in this study were not collected in a protected area. No specific permissions were required for sampling of seawater in the locality. The samples taken for our study did not involve endangered or protected species.

2.1. Experimental setup and sampling

The study was carried out aboard the R/V *Tansei Maru* (JAMSTEC) during the KT-11-7 cruise in May 2011. Water samples were collected from 10-m depth at a station (41° 30' N, 144° 00' E, 1668 m depth, Fig 1) in the Oyashio region of the western North Pacific on 9 May with Niskin-X bottles attached to a CTD-CMS system. A total of 200 L of seawater was poured into four 50 L polypropylene carboys through silicon tubing with 197 μm mesh Teflon nets to remove large particles. Prior to incubation, $FeCl_3$ solution (5 nmol L^{-1} in final concentration) was added to the carboys to promote the development of phytoplankton blooms because the growth of bloom-forming diatoms can be limited by low iron (Fe) availability in this region [45, 46].

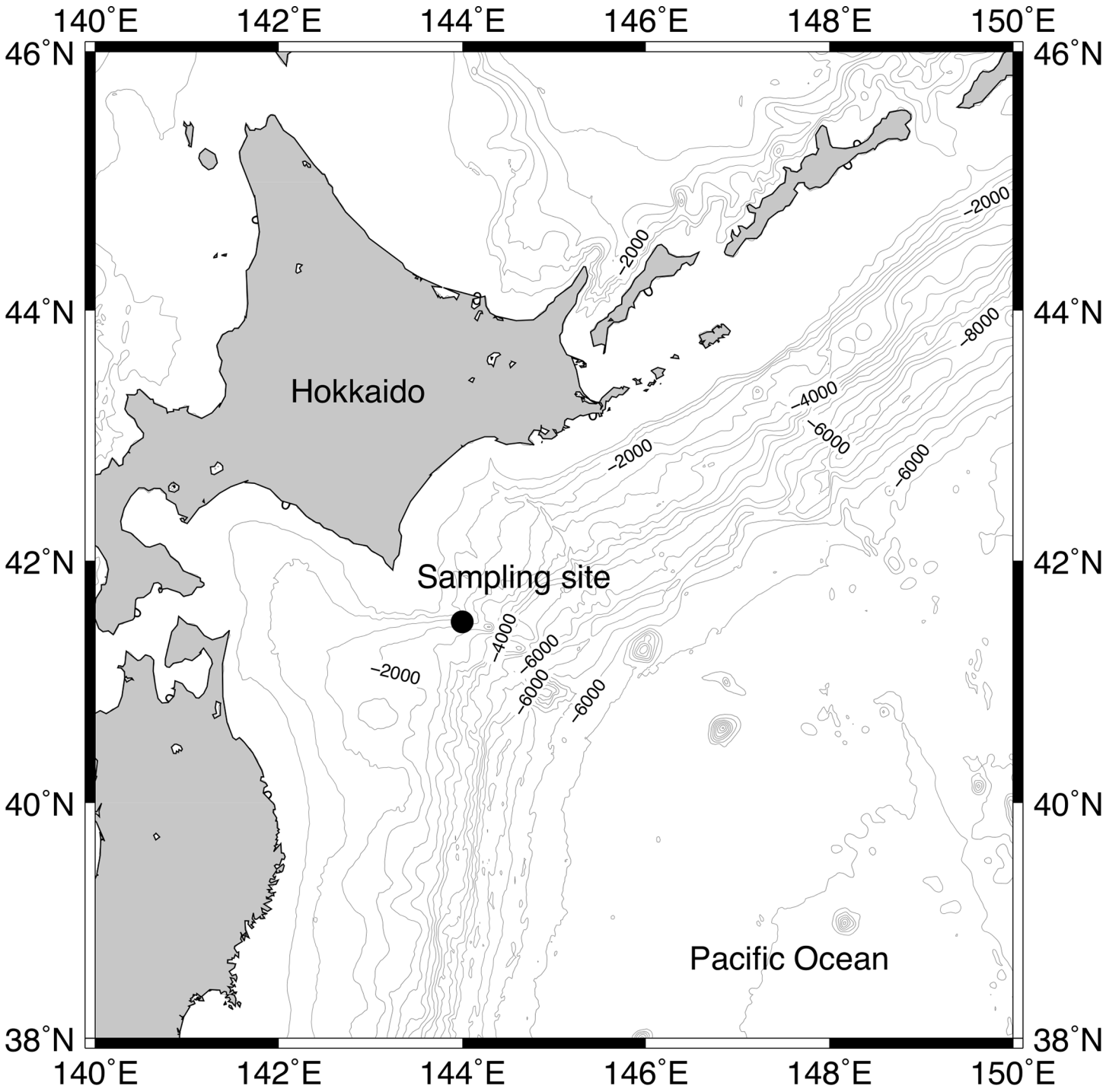

Fig 1. Location of the sampling station (41° 30' N, 144° 00' W) for the incubation experiment.

doi:10.1371/journal.pone.0154291.g001

Subsamples were taken from each carboy and poured into triplicate acid-cleaned 12-L polycarbonate bottles (12 bottles total) for incubation. Initial (day 0) samples were collected from each carboy. Initial seawater pCO_2 (i.e., 350 μatm) was measured using the Non-Dispersive Infra-Red (NDIR) method using a portable CO_2 analyzer (CO2-09, Kimoto Electric), and the

resulting value was used as the control benchmark. To control pCO_2 in the incubation bottles, air mixtures containing 180, 350, 750, and 1000 μatm CO_2 were bubbled into the incubation bottles. The flow rate of the gases was set at 100 mL min^{-1} for the first 24 h, and thereafter maintained at 50 mL min^{-1}. Incubation was conducted on deck in a tank with running surface seawater for 3 days, maintaining *in situ* temperature of 5°C and 50% surface irradiance, which was adjusted using a neutral density screen. The temperature of the incubation tanks ranged between 4.7 and 6.0°C throughout the incubation. All of the samples, except on day 0, were collected between 5:00 and 6:00 a.m.

2.2. Carbonate chemistry, nutrients, and Chl *a* analyses

Samples for total alkalinity (TA), dissolved inorganic carbon (DIC), nutrients, and size-fractionated chlorophyll *a* (Chl *a*) were collected on days 0, 0.6, 1.6, and 2.6 (hereafter days 0, 1, 2, and 3, respectively) from the incubation bottles. Samples for TA and DIC were collected in airtight glass vials and poisoned with $HgCl_2$ prior to their storage at 4°C for analysis on shore. Concentrations of TA and DIC were measured with a total alkalinity analyzer using the potentiometric Gran Plot method (ATT-05, Kimoto Electric) following Edmond [50]. The values of pCO_2 and pH were calculated from the TA and DIC using the CO2SYS program [51]. Nutrient samples were poured into 10 mL plastic tubes and stored at −20°C until they were analyzed on shore. Concentrations of nitrate plus nitrite, nitrite, phosphate, and silicic acid were measured using a QuAATro-2 continuous-flow analyzer (Gran+Luebbe). Size-fractionated Chl *a* samples were collected onto a 10 μm pore size polycarbonate filter without vacuum or onto Whatman GF/F filters under a gentle vacuum (< 0.013 MPa). Pigments were extracted in *N*,*N*-dimethylformamide (DMF; [52]), and Chl *a* concentrations were then determined using a Turner Design fluorometer (model 10-AU) with the non-acidification method of Welschmeyer [53].

2.3. FIRe fluorometry

To obtain the maximum photochemical quantum efficiency (F_v/F_m) of photosystem II (PSII) for phytoplankton in each bottle, a Fluorescence Induction and Relaxation (FIRe) fluorometer (Satlantic) was used. The water samples were collected daily from the incubation bottles and were measured following Sugie et al. [18].

2.4. HPLC and CHEMTAX analyses

Pigment samples for high-performance liquid chromatography (HPLC) were collected on days 0, 2, and 3. The water samples (600–1000 mL) were filtered onto Whatman GF/F filters under a gentle vacuum (< 0.013 MPa), flash-frozen in liquid nitrogen and then stored in a deep freezer (−80°C) until analysis. HPLC pigment analysis was conducted following the method of Endo et al. [16]. The net growth rate (μ, day^{-1}) of each pigment was calculated from the following equation:

$$\mu = \frac{dC}{dt}\left(\frac{1}{C}\right)$$

where C is the pigment concentration (μg L^{-1}) and t is incubation time (i.e., 2.6 days). Based on the chemotaxonomic pigment concentrations, phytoplankton community structure was estimated using the CHEMTAX program [54] following Endo et al. [16]. The initial and final matrices of pigment:Chl *a* ratios are shown in S1 and S2 Tables, respectively.

2.5. qPCR and qRT-PCR

Samples for DNA and RNA analyses were collected on days 0, 2 and 3. DNA samples (300–400 mL) were collected onto 0.2 μm pore size polycarbonate Nuclepore membrane filters (Whatman) with gentle vacuum (< 0.013 MPa), flash frozen in liquid nitrogen and then stored in a deep freezer at −80°C until analysis. Seawater samples (300–400 mL) for RNA analysis were filtered onto 0.2 μm pore size polycarbonate Nuclepore filters (Whatman) with gentle vacuum (< 0.013 MPa) and then stored in 1.5-mL cryotubes previously filled with 0.2 g of muffled 0.1-mm glass beads and 600 μL of RLT buffer (Qiagen) with 10 μL mL^{-1} β-mercaptoethanol (Sigma-Aldrich). The RNA samples were flash-frozen in liquid nitrogen and stored in a deep freezer at −80°C until analysis. The detailed methodologies of total DNA and RNA extractions were described in Endo et al. [16] and Endo et al. [27], respectively. The extracted RNA was reverse-transcribed into cDNA using the PrimeScript RT Reagent Kit with gDNA Eraser (Takara). To quantify the diatom-specific *rbcL* gene (DNA) and its transcripts (cDNA), qPCR and qRT-PCR were performed according to the method of Endo et al. [27].

2.6. Ion Torrent Personal Genome Machine (PGM) sequencing

Gene fragments of diatom-specific *rbcL* sequences were amplified from the extracted DNA or cDNA samples with barcoded fusion primer pairs, which included the primer set designed by John et al. [55]: forward primer, 5'-GATGATGARAAYATTAACTC-3'; reverse primer, 5'-TA WGAACCTTTWACTTCWCC-3'. The forward primer included the A-adaptor (5'-CCA TCTCATCCCTGCGTGTCTCCGAC-3'), key (5'-TCAG-3') and multiplex identifier (MID) sequences set by the manufacturer (Life Technologies), whereas the reverse primer included the truncated Pi-adapter (trP1: 5'-CCTCTCTATGGGCAGTCGGTGAT-3') sequence. Triplicate PCR amplifications were conducted for each samples using the TaKaRa Ex *Taq* Hot Start Version (Takara). The thermal cycling conditions were 60 s at 94°C for initial denaturation, then 30 cycles consisting of 10 s at 98°C, 30 s at 52°C, and 60 s at 72°C, followed by 10 min at 72°C for final extension. The PCR amplification was checked with 1.5% agarose gel electrophoresis. Amplicons were purified using AMPure beads (Beckman Coulter) and then quantified by an Agilent 2100 Bioanalyzer using the DNA 1000 Kit (Agilent Technologies) following the manufacturer's instructions. Then, the PCR templates were diluted to the final concentration of 26 pmol L^{-1}, and these were mixed equally in terms of concentration. Emulsion PCR was performed using an Ion One Touch 2 system with Ion PGM Template OT2 200 kit (Life Technologies) according to the manufacturer's protocol. The emulsion PCR products were enriched using an Ion One Touch ES (Life Technologies) and then loaded onto an Ion 318 v2 chip (Life Technologies). Sequencing of the amplicon libraries was performed using an Ion Torrent PGM system with the Ion PGM sequencing 200 kit v2 (Life Technologies) according to the manufacturer's protocol.

2.7. Sequence analyses

2.7.1. Quality filtering. Sequences with low quality, polyclonal sequences, and sequences that did not match against the A-adapter were initially filtered out with the Torrent Suite Software (Life Technologies), and the data so obtained were exported as FASTQ files. The complete run files in each sample were deposited in the DDBJ Sequence Read Archive (DRA) with the accession number DRA003722. Additional quality controls were performed using the software FASTX-Toolkit (http://hannonlab.cshl.edu/fastx_toolkit/). Sequencing reads were excluded if they met any of the following criteria: (i) reads not containing the trP1 adapter sequence; (ii) reads not matching the reverse primer sequence; (iii) reads shorter than 112 bp; and (iv) reads

with average quality score below 25. Sequence quality statistics of raw and quality-filtered libraries are shown in S3 Table.

2.7.2. Taxonomic assignment. For taxonomic classification, contig assembly was achieved using the software SeqMan NGen (DNASTAR). Fifty thousand reads for each library were assembled into contigs with ≥ 97% sequence identity. The representative sequences of each contig containing with ≥ 100 reads (≥ 0.2% for total reads) were compared with *rbcL* sequences deposited in GenBank database (http://www.ncbi.nlm.nih.gov) using the BLAST query engine. Contigs that have ≥ 93% sequence similarity with known *rbcL* sequences were classified into the following groups: Chaetocerotaceae, Coscinodiscaceae, Cymatosiraceae, Rhizosoleniaceae, Stephanodiscaceae, Thalassiosiraceae, Achananthaceae, Bacillariaceae, Naviculaceae, Fragilariaceae, unidentified diatoms, and other eukaryotes. Contigs related to two or more diatom families with the same sequence similarity were assigned as unidentified diatoms. Other eukaryotes consisted of the contigs that were closely related to the sequences from organisms other than diatoms deposited in GenBank. A phylogenetic tree constructed with *rbcL* reference sequences is shown in S4 Fig.

2.7.3. Sequence-based statistical analyses. Principal Component Analysis (PCA) was used to recognize the relationships among pCO_2 levels in the DNA or cDNA libraries by reducing the multivariate information using the software R (http://www.r-project.org/). The ordination was performed based on the matrix of relative compositions at the family level in the libraries. In addition, ten thousand reads in each library were extracted for diversity analyses by the software mothur v. 1.25.0 [56]. All libraries were merged and clustered into operational taxonomic units (OTUs) with ≥ 97% sequence similarity cutoff. Singleton OTUs were then removed from the libraries. Genetic diversity was assessed based on the number of OTUs, Shannon-Wiener index (*H*', [57]), and Simpson's index (1-*D*, [58]).

2.8. Significance test

Statistical analyses were performed with the software R (http://www.r-project.org). To evaluate the statistically significant differences among CO_2 treatments, Kruskal-Wallis one-way analysis of variance (ANOVA) was used. Holm's test for multiple comparisons was also used to identify the source of variance. For all tests, $p < 0.05$ was considered significant.

Results

3.1. Carbonate chemistry and nutrients

The initial concentrations of TA and DIC in the seawater were 2239.4 and 2074.7 μmol kg^{-1}, respectively (Table 1). Initial values of calculated pH and pCO_2 were 8.1 and 333.1 μatm, respectively (Table 1). Our incubation system successfully created significant gradients in pCO_2 and pH (S1 Fig) in seawater without any variation in TA between CO_2 treatments. Significant gradients in pCO_2 were achieved within 0.6 days, and it took at least 1.5 days to reach the intended pCO_2 values (S1A Fig). The mean pCO_2 values after day 2 in the 180, 350, 750, and 1000 μatm CO_2 treatments were 232, 328, 628, and 822 μatm, respectively. The initial concentrations of nitrate, phosphate, and silicic acid in seawater were 13.72, 0.99, and 11.76 μmol L^{-1}, respectively, and the macronutrients remained until the end of the incubation (Table 1).

3.2. Chl *a* and F_v/F_m

The initial concentration of Chl *a* was 0.70 μg L^{-1} (≥ 10 μm: 0.18 μg L^{-1}, GF/F (ca. 0.7 μm) −10 μm: 0.52 μg L^{-1}). Concentrations of Chl *a* increased over time and reached a maximum at the end of the incubation (Table 2, S2 Fig). Although there was no significant difference in Chl

Table 1. Carbonate chemistry and nutrient concentrations (value ± 1 SD, n = 3, except for the initial: n = 4) at the initial (day 0) or end (day 3) of the incubation.

	TA	DIC	pCO_2	pH	Nitrate	Phosphate	Silicic acid
	(μmol kg^{-1})	(μmol kg^{-1})	(μatm)	(Total scale)	(μmol L^{-1})	(μmol L^{-1})	(μmol L^{-1})
Initial	2239.4 ± 1.2	2074.7 ± 0.9	333.1 ± 1.9	8.10 ± 0.00	13.72 ± 0.04	0.99 ± 0.03	11.76 ± 0.05
180 μatm	2245.3 ± 0.4	2014.9 ± 2.0	225.6 ± 2.9	8.25 ± 0.00	13.22 ± 0.04	0.99 ± 0.01	11.06 ± 0.04
350 μatm	2243.6 ± 2.3	2078.5 ± 1.2	333.2 ± 3.6	8.10 ± 0.00	13.13 ± 0.02	1.00 ± 0.00	10.99 ± 0.06
750 μatm	2245.6 ± 1.2	2172.2 ± 0.8	645.6 ± 1.6	7.84 ± 0.00	13.26 ± 0.01	1.02 ± 0.00	11.27 ± 0.07
1000 μatm	2245.0 ± 0.7	2202.9 ± 2.7	839.9 ± 15.8	7.73 ± 0.01	13.28 ± 0.01	1.01 ± 0.01	11.19 ± 0.06

doi:10.1371/journal.pone.0154291.t001

a concentration in the small (GF/F–10 μm) fraction among samples incubated at different CO_2 levels during the sampling period, the Chl *a* concentration in the large (≥10 μm) fraction was significantly lower in the high (750 and 1000 μatm) CO_2 treatments than in the control (350 μatm) treatment on day 3 (Kruskal-Wallis ANOVA, Holm's test, $p < 0.05$).

Initial values of F_v/F_m were ca. 0.38 (Table 2, S3 Fig). The values of F_v/F_m increased to ca. 0.44 for all treatments on day 1 and remained above 0.41 until the end of the incubation. The F_v/F_m values of samples incubated under different CO_2 levels were not significantly different (Kruskal-Wallis ANOVA, $p > 0.05$).

3.3. Phytoplankton pigments

In the initial seawater, the concentrations of fucoxanthin (Fuco) and alloxanthin (Allo), which are biomarkers of diatoms in the Oyashio region during spring [47] and of cryptophytes [59], respectively, were relatively high among the carotenoids detected in this study. During incubation, the net growth rates of Fuco were the highest among all of the chemotaxonomic pigments in all of the incubation bottles (Fig 2). Significant differences in the net growth rates of Fuco were found among the CO_2 treatments (Kruskal-Wallis ANOVA, $p < 0.05$), and the value for the control treatment was higher than that for the other treatments (Holm's test, $p < 0.05$) (Fig 2). The net growth rates of Chl *a* and Allo were not significantly different among the CO_2 treatments (Kruskal-Wallis ANOVA, $p > 0.05$).

The initial phytoplankton community was mainly dominated by cryptophytes and diatoms (38.1% and 34.8% contributions to the Chl *a* biomass, respectively) (Fig 3). Contributions of diatoms to the Chl *a* biomass increased (> 47% in all CO_2 treatments on day 3), whereas those of cryptophytes decreased (< 30%). The diatom contributions in the high-CO_2 treatments are significantly lower than those in the low or control CO_2 treatments on day 3 (Kruskal-Wallis ANOVA, Holm's test, 180 and 350 μatm > 750 and 1000 μatm, $p < 0.05$). On the other hand, contributions of cryptophytes, haptophytes, and pelagophytes to Chl *a* biomass were

Table 2. Size-fractionated Chl *a* and F_v/F_m parameters (value ± 1 SD, n = 3, except for the initial: n = 4) at the initial (day 0) or end (day 3) of the incubation.

	Small-sized Chl *a*	Large-sized Chl *a*	F_v/F_m
	(μg L^{-1})	(μg L^{-1})	(Relative)
Initial	0.52 ± 0.03	0.18 ± 0.04	0.38 ± 0.01
180 μatm	0.89 ± 0.01	0.60 ± 0.08	0.43 ± 0.01
350 μatm	0.87 ± 0.01	0.70 ± 0.02	0.44 ± 0.01
750 μatm	0.85 ± 0.02	0.49 ± 0.02	0.41 ± 0.01
1000 μatm	0.87 ± 0.00	0.51 ± 0.03	0.41 ± 0.01

doi:10.1371/journal.pone.0154291.t002

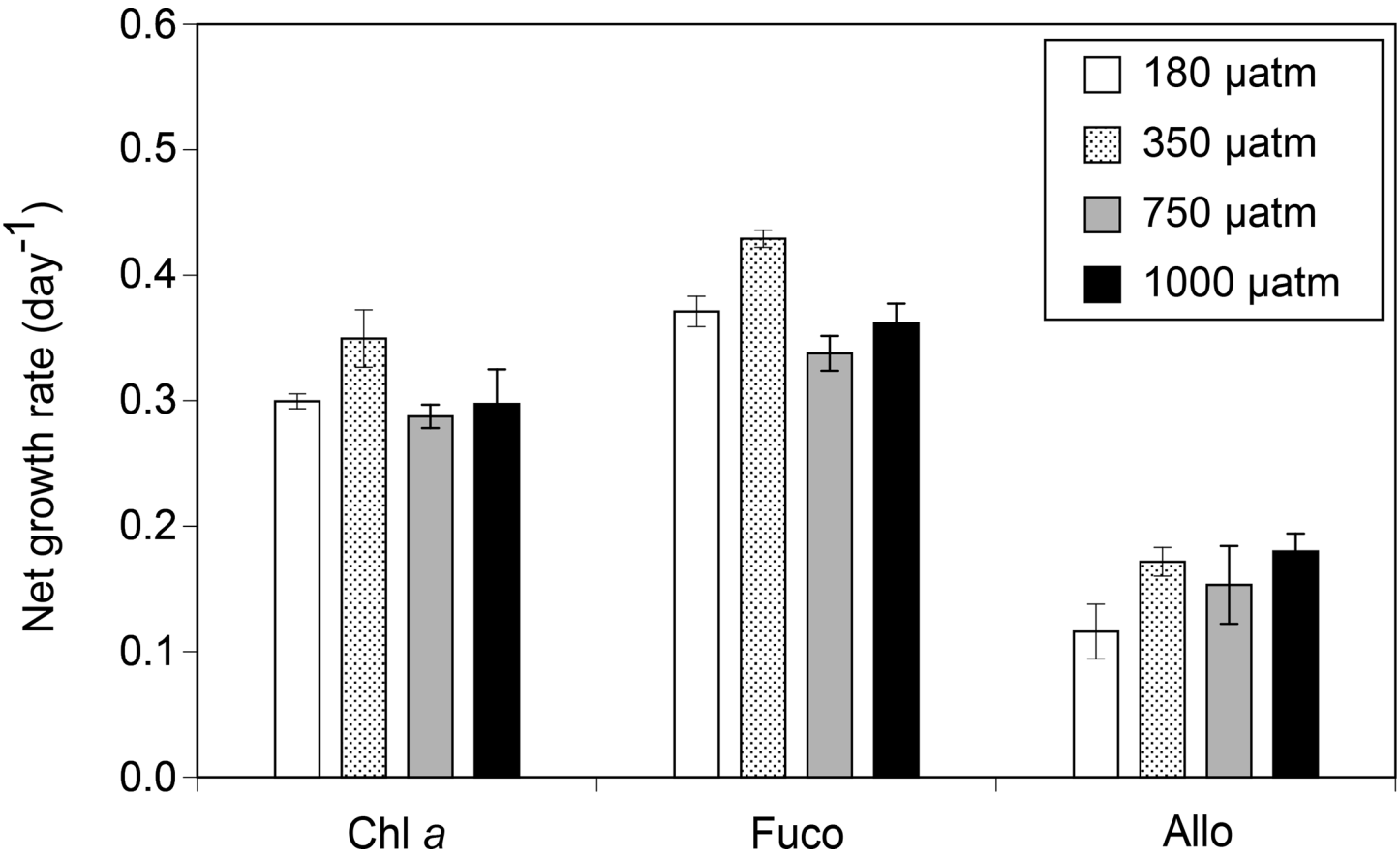

Fig 2. Net growth rates of chlorophyll *a* (Chl *a*), fucoxanthin (Fuco), and alloxanthin (Allo) concentrations as estimated by HPLC during the incubation. Error bars denote ± 1 SD (n = 3).

doi:10.1371/journal.pone.0154291.g002

significantly higher in the high-CO_2 treatments on day 3 (Kruskal-Wallis ANOVA, Holm's test, 180 and 350 µatm < 750 and 1000 µatm, $p < 0.05$).

3.4. Copy numbers of *rbcL* DNA and cDNA of diatoms

A significant positive correlation between Fuco concentration and the diatom-specific *rbcL* gene copy count was found during the incubation ($R^2 = 0.910$, $p < 0.001$, $n = 25$) (Fig 4). In addition, a significant negative correlation was found between seawater pCO_2 and diatom-specific *rbcL* cDNA copy count on day 3 ($R^2 = 0.506$, $p < 0.01$, $n = 12$) (Fig 5A). However, no significant correlation existed between the seawater pCO_2 and the diatom-specific *rbcL* cDNA abundance normalized to the DNA abundance (cDNA/DNA) on day 3 ($R^2 = 0.035$, $p > 0.05$, $n = 9$) (Fig 5B).

3.5. Molecular OTU-based analyses of diatom-specific *rbcL* DNA and cDNA

The sequence data ranged from 340,809 to 1,194,481 reads per sample were generated from the Torrent Suite software, and approximately 80% of the raw sequences were removed by the subsequent procedures (S3 Table). As a result of the data filtering, average quality score of our sequence data increased from ca. 27.7 to ca. 31.4, indicating that the average error rate of our libraries was below 0.1%. The rarefaction curves plateaued when 10,000 sequences were

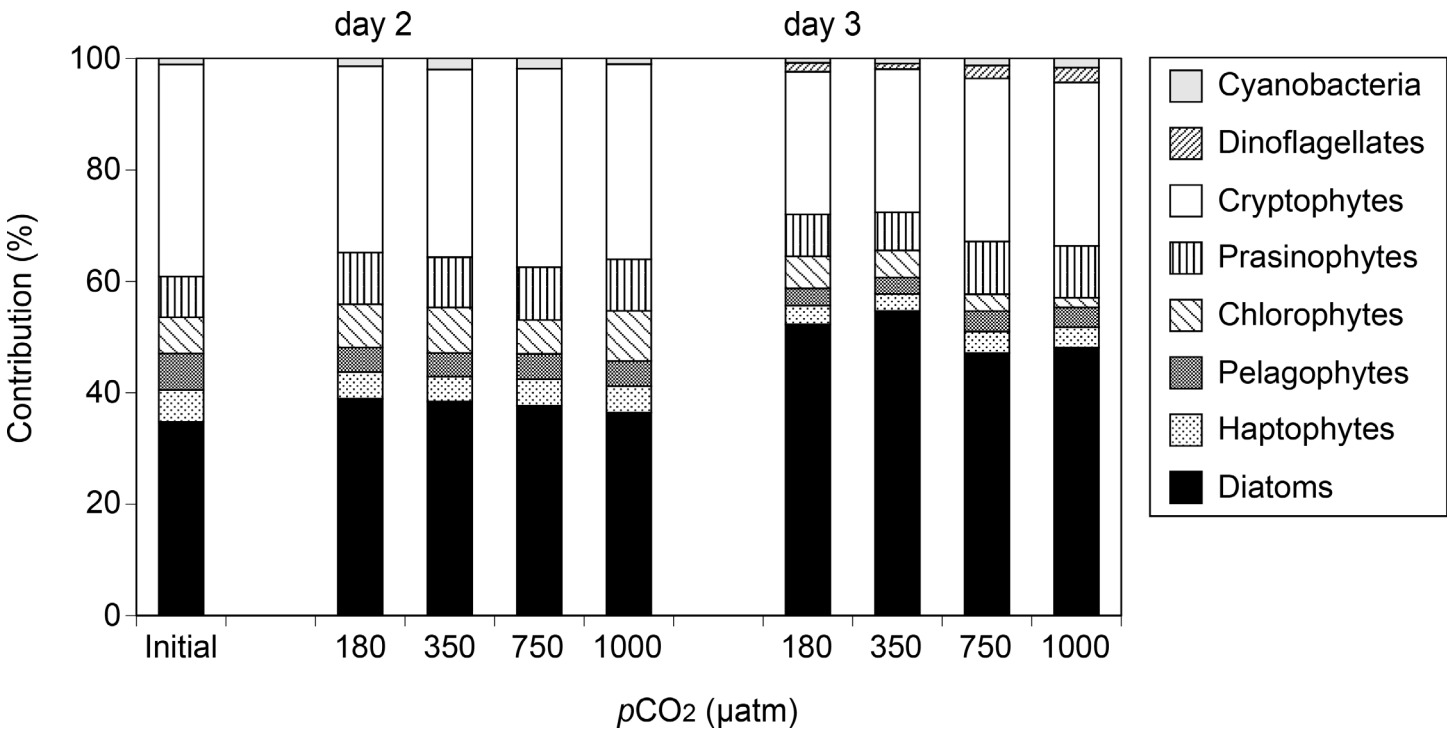

Fig 3. Mean contributions of each phytoplankton group to total Chl *a* biomass as estimated by CHEMTAX. Error bars denote ± 1 SD (n = 3).

doi:10.1371/journal.pone.0154291.g003

calculated for each treatment (S5 Fig). The NGS libraries of diatom-specific *rbcL* DNA and cDNA from the initial sample contain 117 and 113 OTUs, respectively (Table 3). On day 0, genetic diversity in the DNA library, calculated using the Shannon and Simpson indices, was 2.30 and 0.772, for *H*' and 1-*D*, respectively. Similarly, those in the cDNA library were 2.50 and 0.829, respectively. At the end of the incubation, the highest OTU values and diversity indices were observed in the control treatment in the DNA and cDNA libraries (Table 3). The values of *H*' and 1-*D* were significantly higher in the 180 and 350 µatm CO_2 treatments than in the 750 and 1000 µatm CO_2 treatments on day 3 (*t*-test, $p < 0.05$).

For the DNA and cDNA libraries, more than 85% of the sequences were closely related to the known diatom sequences with ≥ 93% sequence similarity. In the initial seawater, the dominant diatom groups in the *rbcL* DNA were Bacillariaceae and Fragilariaceae (52.0% and 18.3%, respectively), followed by unidentified diatoms, Chaetocerotaceae, Thalassiosiraceae, and Coscinodiscaceae (5.6%, 3.7%, 3.4%, and 1.9%, respectively) (Fig 6A). Initial *rbcL* cDNA consisted mainly of Bacillariaceae and Chaetocerotaceae (43.8% and 15.0%, respectively), followed by unidentified diatoms, Fragilariaceae, Coscinodiscaseae and Thalassiosiraceae (12.4%, 11.0%, 3.2% and 2.9%, respectively) (Fig 6B). At the end of the incubation, the contributions of Thalassiosiraceae and Fragilariaceae to the total population increased relative to the initial contribution for all of the CO_2 treatments in the DNA and cDNA libraries (Fig 6). The contributions of Bacillariaceae to the total became higher in the 180, 750 and 1000 µatm CO_2 treatments compared with the control (Fig 7A and 7B). On the other hand, the contributions of Fragilariaceae, Thalassiosiraceae, and Chaetocerotaceae to the total decreased in the 180, 750 and 1000 µatm CO_2 treatments relative to the control on day 3. Percent differences in Bacillariaceae, Fragilariaceae, Thalassiosiraceae, and Chaetocerotaceae were higher in the cDNA than in the DNA. The contributions of Coscinodiscaceae to the total population increased in the low CO_2 treatment relative to the control in both the DNA and cDNA libraries on day 3.

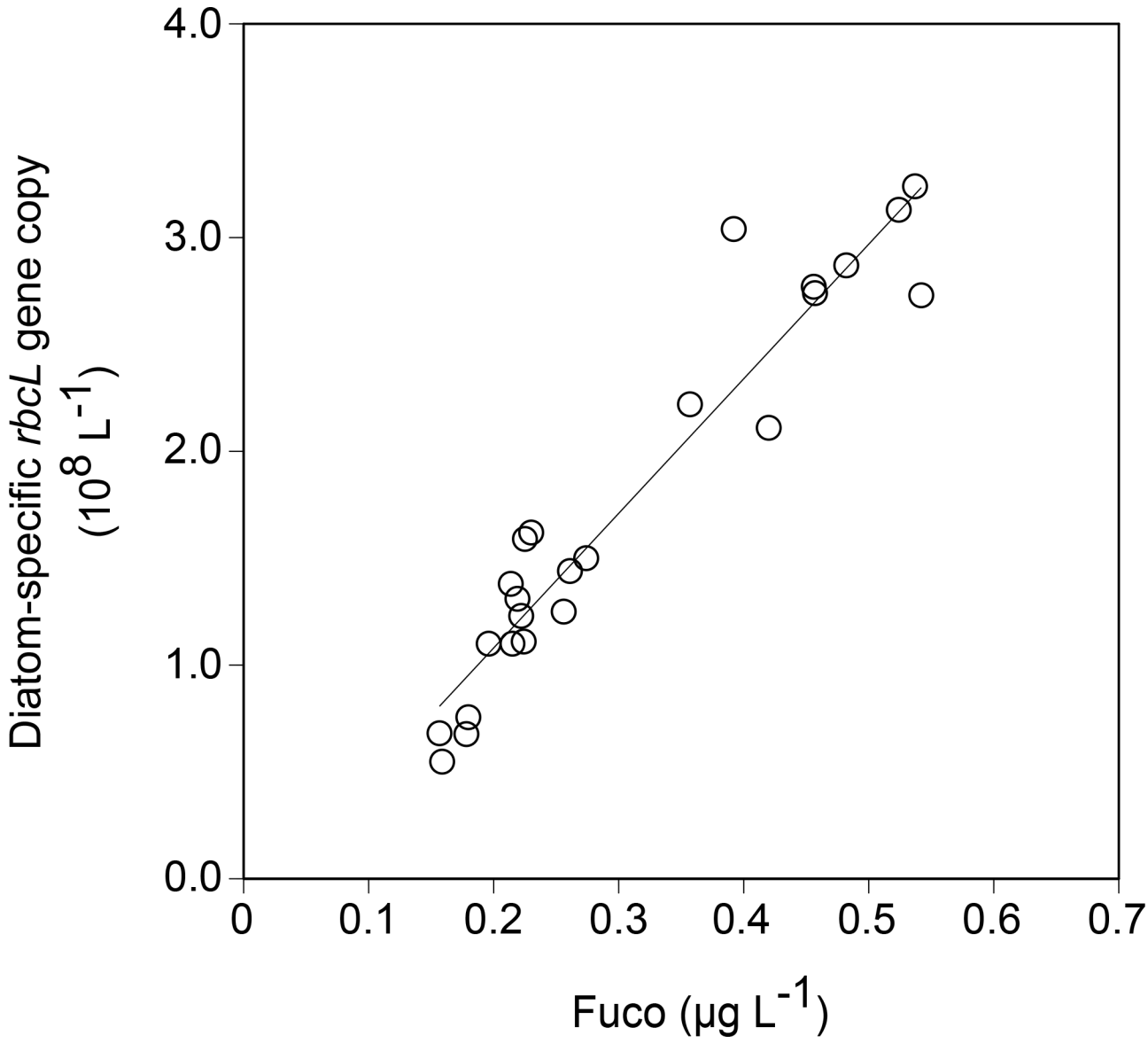

Fig 4. Relationship between fucoxanthin (Fuco) concentration and diatom-specific *rbcL* copy number ($y = 6.29\times10^8x - 1.90\times10^8$, $R^2 = 0.910$, $p < 0.001$, n = 25).

doi:10.1371/journal.pone.0154291.g004

In the PCA plot (Fig 8), libraries were divided into DNA and cDNA by the first axis (PC1), and these were further divided to high (750 and 1000 μatm) and other (180 and 350 μatm) CO_2 treatments by the second axis (PC2), except for the 750 μatm CO_2 treatment in the DNA library. In the PCA analysis, the first and second axes from the ordination explained 50.5% and 27.6% of the total variability, respectively (cumulative contribution of 78.1%).

Discussion

4.1. Chemical and biological characteristics of the incubation seawater

In our experiment, initial seawater pCO_2 was intermediate value between pre- and post-bloom phases in the Oyashio region reported by Midorikawa et al. [20]. In addition, in the initial

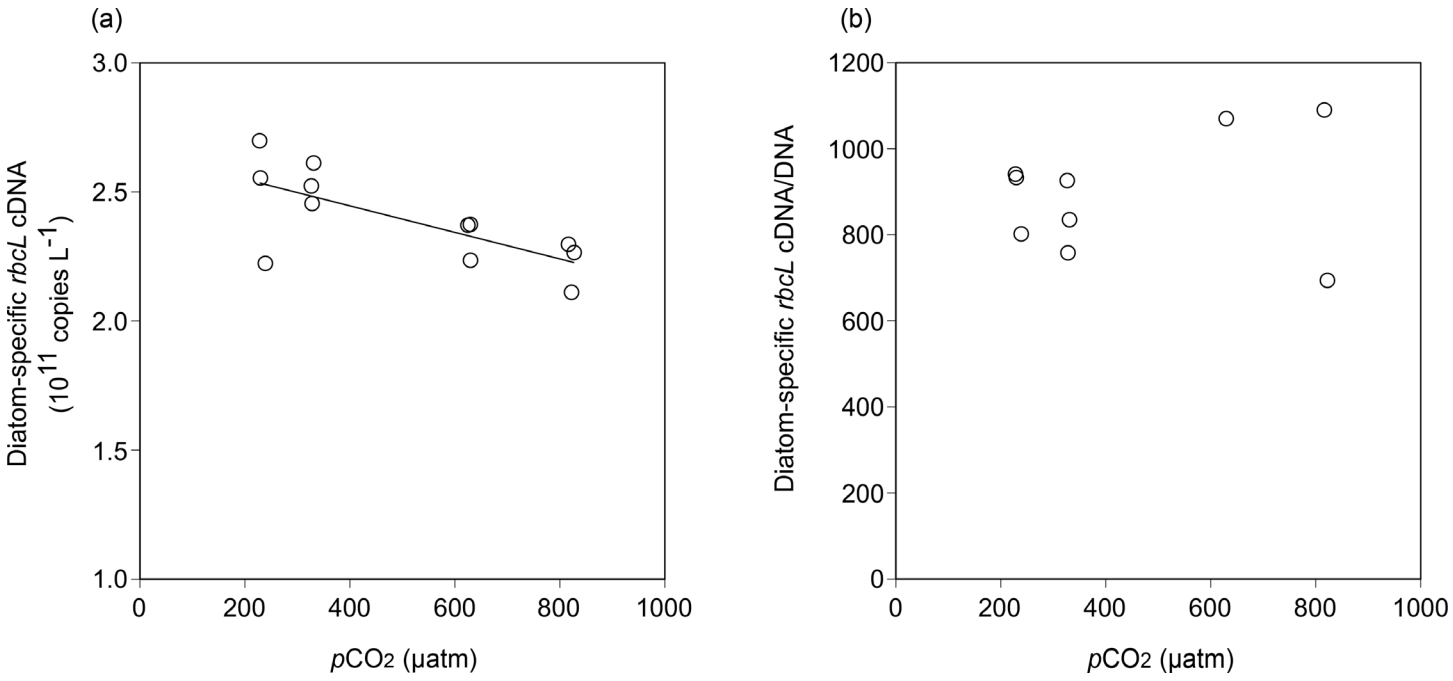

Fig 5. Relationships between seawater pCO_2 (calculated values from TA and DIC) and (a) diatom-specific *rbcL* cDNA copies and (b) diatom-specific *rbcL* cDNA copies normalized to *rbcL* gene copy on day 3.

doi:10.1371/journal.pone.0154291.g005

seawater, macronutrients were not depleted, and the Chl *a* concentration was lower than the values previously reported during the spring diatom blooms in this region (> 5 μg L^{-1}, [20, 47, 60]). These results indicate that the intense diatom bloom has not yet occurred in the seawater used for the incubation experiment. This speculation is supported by our CHEMTAX analysis, which revealed that the initial phytoplankton assemblages were dominated by a mixture of diatoms and cryptophytes (Fig 3) as previously observed during the pre-bloom period [47, 60]. The initial value of F_v/F_m was also similar to that in the pre-bloom phase in spring Oyashio water measured with fast repetition rate fluorometry (FRRF) by Yoshie et al. [61]. Concentrations of Chl *a* increased exponentially during the incubation (S2 Fig) and it was accompanied by the increases in diatom contribution to the Chl *a* biomass (Fig 3), suggesting that our incubation could simulate the early growth phase of the diatom bloom.

4.2. Effects of CO_2 availability on the phytoplankton pigments and F_v/F_m

The net growth rates of Fuco were less in the low (180 μatm) and high (750 and 1000 μatm) CO_2 treatments relative to the control (350 μatm), while no significant CO_2 difference was

Table 3. Number of OTUs and diversity indices (value ± 95% confidence interval) for *rbcL* DNA and cDNA libraries obtained from the initial sample and the incubation bottles on day 3.

	DNA			cDNA		
	OTUs	*H'*	1-*D*	OTUs	*H'*	1-*D*
Initial	117	2.30 ± 0.04	0.772 ± 0.007	113	2.50 ± 0.03	0.829 ± 0.005
180 μatm	95	2.22 ± 0.03	0.753 ± 0.008	95	2.35 ± 0.03	0.808 ± 0.006
350 μatm	114	2.27 ± 0.03	0.759 ± 0.008	103	2.35 ± 0.03	0.809 ± 0.006
750 μatm	103	2.15 ± 0.03	0.740 ± 0.007	95	2.28 ± 0.03	0.785 ± 0.005
1000 μatm	101	2.16 ± 0.03	0.745 ± 0.007	98	2.24 ± 0.03	0.774 ± 0.005

doi:10.1371/journal.pone.0154291.t003

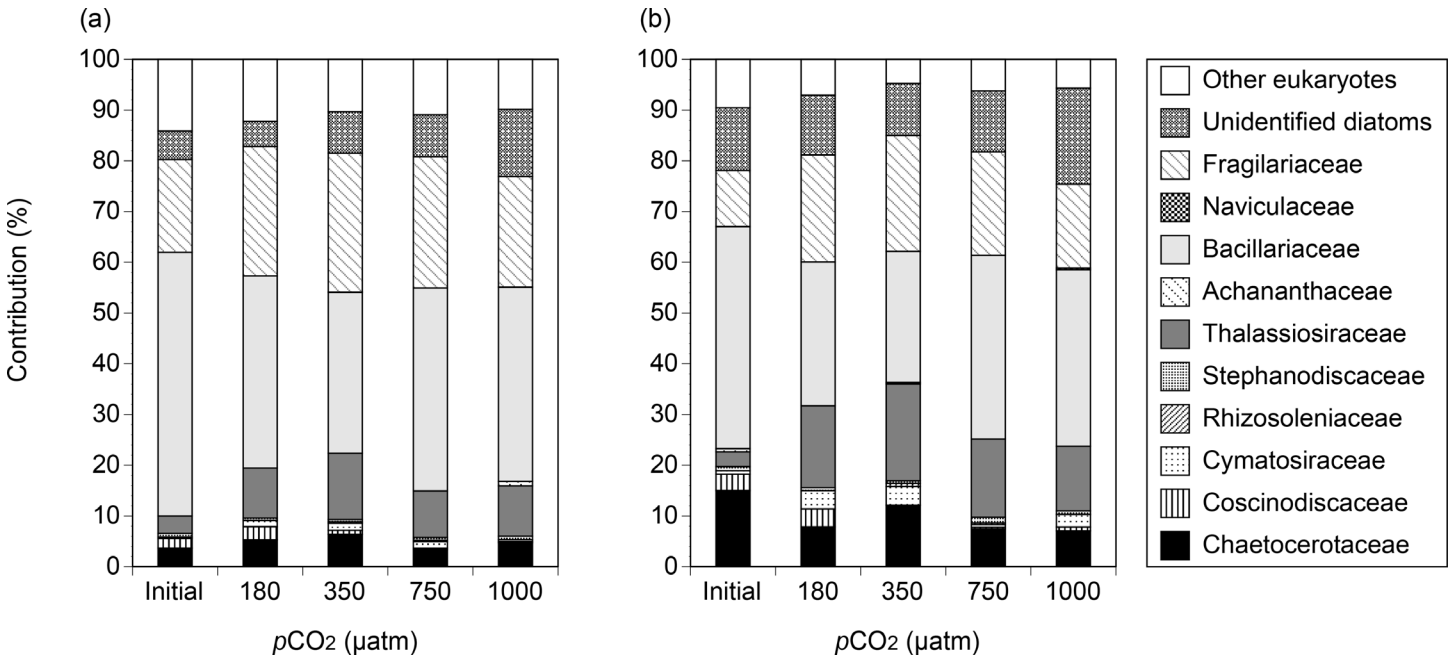

Fig 6. Relative taxonomic contributions (%) in the *rbcL* (a) DNA and (b) cDNA libraries obtained from the initial samples and the 180, 350, 750, and 100 µatm CO_2 treatments on day 3.

doi:10.1371/journal.pone.0154291.g006

observed in the other chemotaxonomic pigments (Fig 2), suggesting that the growth of diatoms could be selectively diminished by changes in CO_2 availability. This assumption is supported by size-fractionated Chl *a* analysis, which showed that elevated CO_2 levels selectively decreased large-sized (≥10 µm) phytoplankton cells, that were most likely composed of diatoms. Our results were inconsistent with the previous laboratory culture experiments, which indicated that diatoms tended to increase their growth under elevated CO_2 levels [10, 11]. In addition, Wu et al. [62] demonstrated that the CO_2 enrichment stimulated the growth of larger diatom species rather than that of smaller cells. However, field studies using natural phytoplankton assemblages showed positive [12, 13, 28] and negative [17, 27, 63] effects of increased CO_2 availability on diatom growth. This pattern may have been caused by differences in diatom species [4, 19, 62], an effect of CO_2 on zooplankton grazing [64], and/or the bioavailability of iron in response to the change in carbonate chemistry [18]. Our findings further support that the sensitivity of phytoplankton assemblages to elevated CO_2 differs geographically, according to the differences in species composition and environmental conditions [5]. In the present study, decreased contributions of diatoms resulted in the relative increases in other phytoplankton taxa, such as cryptophytes and haptophytes (Fig 3). Our results suggest that CO_2 enrichment may decrease the diatom contribution to the phytoplankton assemblages during the growth phase of spring blooms in the Oyashio region. However, it should be noted that our incubation period was short (i.e., 1–2 days under fully manipulated CO_2 conditions) and may not have allowed for full acclimation of phytoplankton community to changes in CO_2. Therefore, the biological responses observed in our study could be transient, and further work with a longer incubation period is also required to refine the results observed in our study.

Differences in F_v/F_m values among treatments were not significant throughout the incubation (S3 Fig), indicating that CO_2 availability had a minimal effect on the photochemical quantum efficiency of PSII for phytoplankton assemblages. Similar results were also obtained from Fe-fertilized field experiments [16, 18].

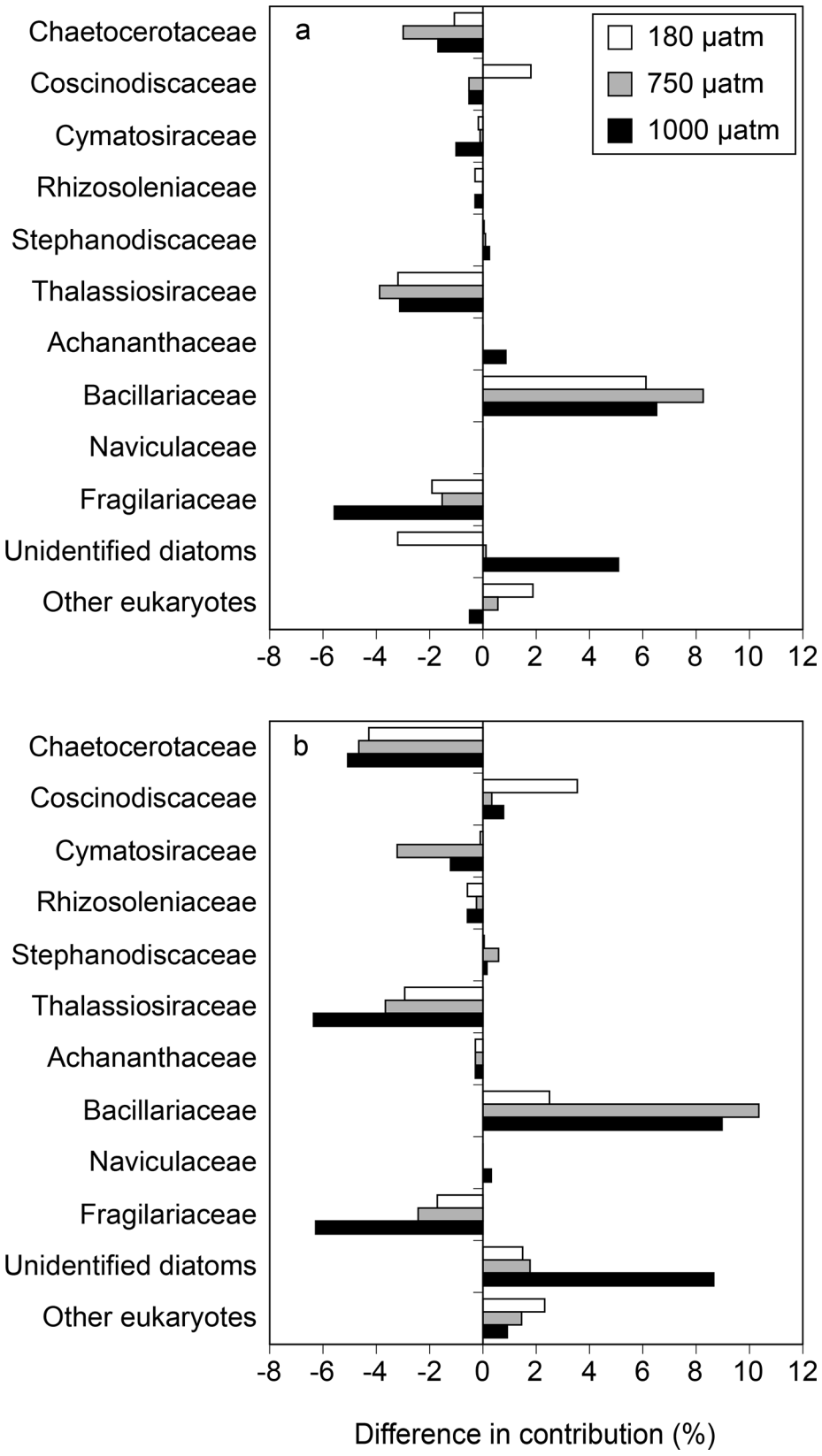

Fig 7. Percent differences in *rbcL* contribution (%) between the control (350 µatm CO_2) and the other pCO_2 treatments in the (a) DNA and (b) cDNA libraries.

doi:10.1371/journal.pone.0154291.g007

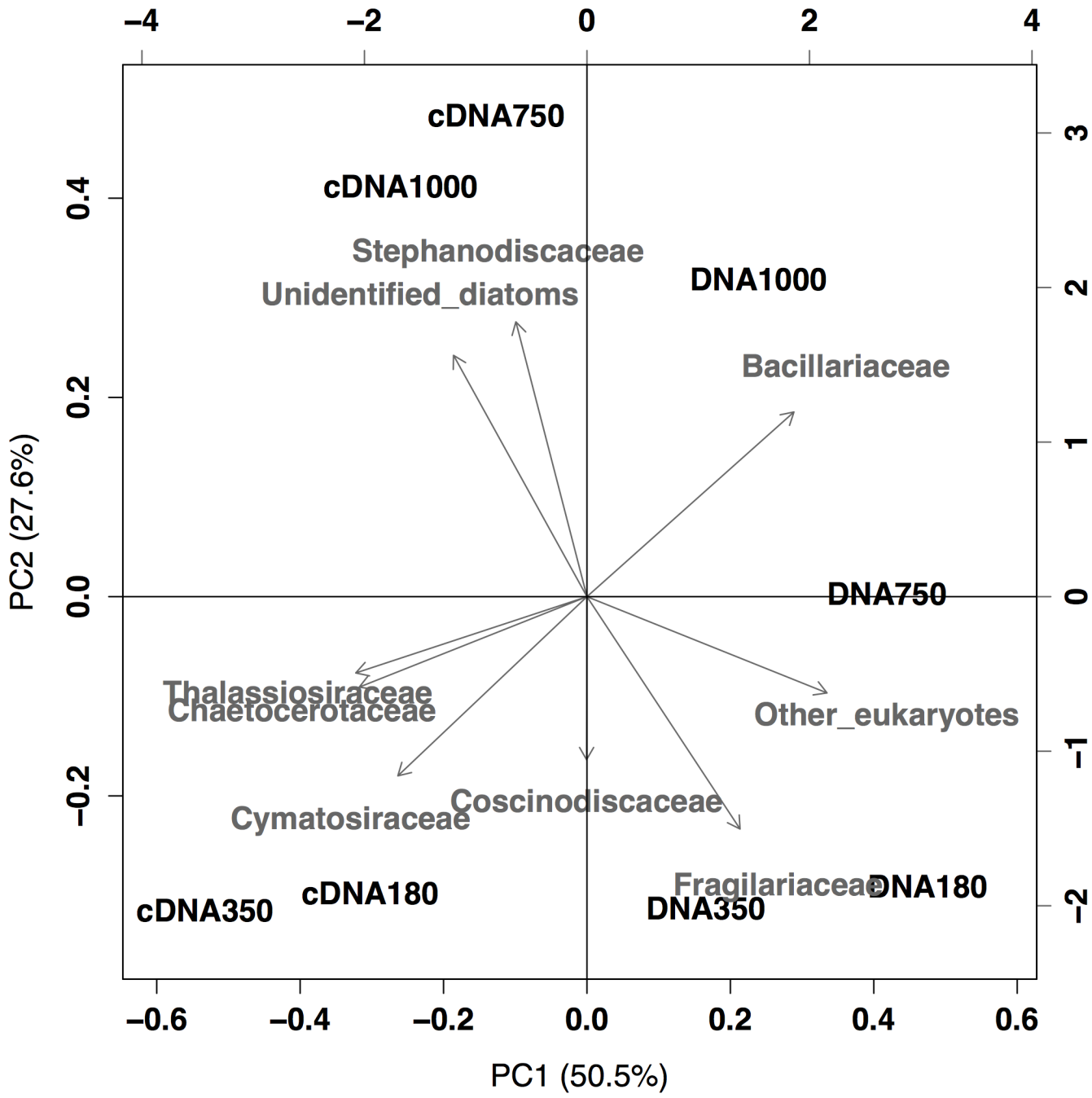

Fig 8. Principal component analysis (PCA) ordination plots incorporating relative contribution of sequence reads for pCO_2 treatments in the DNA and cDNA libraries on day 3. Each sample is represented as the library type followed by the pCO_2 treatments (i.e., DNA180 indicates the DNA sample from the 180 μatm CO_2 treatment).

doi:10.1371/journal.pone.0154291.g008

4.3. Effects of CO_2 availability on the diatom-specific *rbcL* gene and its transcripts

The copy number of *rbcL* gene targeting diatoms exhibited a good correlation with Fuco concentration in this study (Fig 4). This indicates a close coupling between *rbcL* gene and the chemotaxonomic pigment in diatoms. A similar result was also observed during the CO_2-

controlled incubation experiment in the oceanic Bering Sea [27]. Given that Fuco can be a strong indicator of diatom carbon biomass in the Oyashio region [47], our result suggests that the diatom-specific *rbcL* gene could also serve as a potential indicator for diatom carbon biomass in the area.

The abundance of diatom *rbcL* gene transcripts decreased with an increase in pCO_2 (Fig 5A), indicating that RubisCO expression could decrease in high CO_2 environments. However, DNA-normalized *rbcL* transcription did not vary as a function of pCO_2 level, indicating that the transcriptional activity was unaffected by CO_2 availability. Pigment analysis by HPLC also indicated the decrease in diatom biomass under high CO_2 conditions (Figs 2 and 3). Therefore, the decrease in *rbcL* transcript abundance in diatom community might be caused primarily by the decrease in diatom biomass rather than the decrease in transcriptional activity in diatom cells. A laboratory culture experiment using the diatom *Thalassiosira weissflogii* also showed a decrease in RubisCO concentration with an increase in CO_2 concentration over a range of 182 to 750 ppm [65]. Decreases in *rbcL* transcripts or RubisCO concentrations under elevated CO_2 conditions were also observed from the field incubation experiments conducted off the coast of California [65] and in the Bering Sea [27]. However, there is little evidence on CO_2-induced transcriptional regulation of *rbcL* in diatom cells. Moreover, Losh et al. [65, 66] demonstrated that the growth and productivity of phytoplankton assemblages were not affected by increased CO_2 level, although the RubisCO expression decreased. Their study suggested that the decrease in RubisCO content could be compensated by an increase in CO_2 concentration around RubisCO at higher CO_2 levels. In our study, therefore, the decrease in diatom growth rate under high CO_2 levels might be unrelated to the transcriptional response of *rbcL* gene. One possible mechanism for the decrease in diatom biomass is that the increase in photoinhibition under elevated CO_2 levels [62]. The shift in diatom community composition could also affect the abundance of diatom-specific *rbcL* and its transcripts (Fig 7).

Although our results cannot extrapolate to longer-term behaviors in the study area, short-term incubation may be suitable for determining physiological responses in the natural phytoplankton assemblages, because that can reduce artifacts derived from incubation (i.e., so-called bottle effects; [67, 68]). In addition, environmental parameters other than CO_2 (e.g., nutrient availability) would be differentiated among CO_2 treatments after longer incubation period [16, 69], and that complicated the source of the algal responses.

Our rarefaction curves reached plateaus with 10,000 reads for all samples (S5 Fig), suggesting that the sequencing efforts were sufficient to address the comparative analyses among libraries. Taxonomic analysis based on NGS revealed that community composition of *rbcL* gene and its transcripts differed largely among CO_2 treatments on day 3. The result suggests that the diatom community structure shifted rapidly in response to changes in CO_2 levels, whereas transcriptional activity of total diatom community was little affected by CO_2 availability. In our NGS libraries, CO_2-induced changes in the taxonomic composition of diatoms exhibited similar trends between DNA and cDNA. For example, the contributions of Chaetocerotaceae, Thalassiosiraceae, and Fragilariaceae consistently decreased in both the DNA and cDNA libraries in response to changes in CO_2 levels compared to the control, whereas those of the Bacillariaceae increased (Fig 7). A possible explanation for the consistency is that the decrease and increase in *rbcL* transcription could be caused by the decrease and increase in *rbcL* gene abundance, respectively. Our results indicate that the effects of CO_2 availability could differ among diatom taxa, resulting in changes in the community composition.

Elevated CO_2 availability decreased the OTU richness and diversity of diatom-specific *rbcL* genes and their transcripts in our experiment (Table 3). Although the decreases in diversity indices were rather small, the diatom community lost 5–10% in terms of the *rbcL* OTU richness during the incubation. The PCA ordination revealed that the *rbcL* libraries were clearly

separated by high and low CO_2 treatments in both DNA and cDNA libraries (Fig 8), suggesting that the decreases in OTU diversity were accompanied with shifts in the diatom-specific *rbcL* composition.

In contrast to elevated CO_2 treatments, the diversity, taxonomic composition, and transcription activity of diatom-specific *rbcL* were weakly affected by decreases in CO_2 availability (Table 3, Figs 5 and 8), indicating that the diatom community in the study area was rather stable to low CO_2 conditions compared with higher CO_2 conditions. Previous field observations also showed that the diversity and productivity of diatom assemblages were maintained during the spring blooms in the Oyashio region [47, 61]. Our results suggest that the dominant diatom species during the spring blooms in this region could be acclimated to the bloom-induced low CO_2 conditions every spring [20], whereas they may not acclimate well to a high CO_2 environment that had not been experienced before. The acclimation would be accomplished by the use of CCMs mediated by the enzyme carbonic anhydrase (CA; [21, 22]). Burkhardt et al. [70] reported that the activity of CA increased in the low CO_2 (36–180 μatm) treatments compared to the ambient (360 μatm) treatment. Furthermore, it has been proposed that bloom-forming diatom species possess highly efficient and tightly regulated CCMs to maintain their growth even under low CO_2 environments [71]. However, decreases in the growth rate of Fuco and the number of *rbcL* OTUs observed in the low CO_2 treatment, implying that some diatom clades could not respond to abrupt decrease in CO_2 availability. Because there is inter-specific variation in the activity and plasticity in CCMs among diatoms [72, 73], one possible explanation of our results is that diatom species with low CCM capacity were eliminated in the low CO_2 treatments.

Conclusions

In the present study, we focused on the effects of different CO_2 availability on the growth, community composition, and photosynthetic capacity of diatoms in the spring Oyashio waters of the western North Pacific. The comprehensive NGS analyses for the diatom-specific *rbcL* gene and its transcripts enabled us, for the first time, to detect significant changes in taxonomic composition and diversity of diatoms among CO_2 treatments even under the short-term incubation. Consequently, we revealed that the elevated CO_2 availability decreased the OTU richness and diversity of diatom-specific *rbcL* gene and their transcripts. Interestingly, the increase in seawater CO_2 levels reduced the growth rate of diatoms and their relative contribution to the Chl *a* biomass as estimated from photosynthetic pigment signatures. In addition, the transcript abundance of diatom-specific *rbcL* gene also decreased under elevated CO_2 levels. According to Chiba et al. [74], a decrease in springtime Chl *a* concentration accompanied the changes in the predominant diatoms from centrics to pennates during the 1960s and 1990s in the Oyashio region. Additionally, the bloom dynamics could be controlled by physical factors such as the Pacific Decadal Oscillation (PDO, [75]). Therefore, it is crucial to investigate the relationship between environmental changes in Oyashio waters and the dynamics and mechanisms of its spring diatom blooms. We believe that molecular biological techniques can help us to gain a deeper understanding of the changes in the composition and physiology of spring Oyashio diatoms.

Supporting Information

S1 Fig. Temporal changes in (a) pCO_2 and (b) pH. Error bars denote ± 1 SD (n = 2 or 3). (EPS)

S2 Fig. Temporal changes in the concentrations of Chl *a*. Error bars denote ± 1 SD (n = 3). (EPS)

S3 Fig. Temporal changes in F_v/F_m. Error bars denote ± 1 SD (n = 3).
(EPS)

S4 Fig. Neighbor-joining tree based on partial *rbcL* gene reference sequences used for the taxonomic classification. Taxonomic groups are distinguished by different symbols in the tree. Reference sequences which could not be identified as a specific diatom family (i.e., a contig sequence was most closely related to two or more reference sequences that belong to different family) are shown as the gray circle.
(TIFF)

S5 Fig. Rarefaction analysis of the diatom-specific *rbcL* (a) DNA and (b) cDNA libraries of the initial sample and the 180, 350, 750, and 1000 μatm CO_2 treatments on day 3. The rarefaction curves, plotting the number of operational taxonomic units (OTUs) as a function of the number of sequences, were computed by the mothur software package.
(EPS)

S1 Table. Initial pigment:Chl *a* ratios for CHEMTAX analysis: (A) True ratio matrix of Suzuki et al. (2002); (B) double and (C) half the ratios of (A); (D) assigned ratios of 0.75, 0.50 and 0.25 to each element following the method of Latasa (2007).
(DOCX)

S2 Table. Final pigment:Chl *a* ratio matrices obtained by CHEMTAX program.
(DOCX)

S3 Table. Quality statistics of pre- and post-quality control sequence data. Sequence data were obtained from DNA and cDNA samples collected on days 0 and 3.
(DOCX)

Acknowledgments

We wish to thank the captain, officers, and crew of the R/V *Tansei Maru* for their assistance during the cruise. We also thank the editor and anonymous referees for their helpful comments and suggestions.

Author Contributions

Conceived and designed the experiments: HE K. Sugie TY K. Suzuki. Performed the experiments: HE K. Sugie TY K. Suzuki. Analyzed the data: HE K. Sugie. Contributed reagents/materials/analysis tools: HE K. Sugie TY K. Suzuki. Wrote the paper: HE K. Sugie TY K. Suzuki. Organized the research cruise: K. Suzuki.

References

1. Caldeira K, Wickett ME. Anthropogenic carbon and ocean pH. Nature. 2003; 425: 365. PMID: 14508477
2. Doney SC, Fabry VJ, Feely RA, Kleypas JA. Ocean acidification: the other CO_2 problem. Ann Rev Mar Sci. 2009; 1: 169–192. PMID: 21141034
3. Riebesell U, Zondervan I, Rost B, Tortell PD, Zeebe RE, Morel FM. Reduced calcification of marine plankton in response to increased atmospheric CO_2. Nature. 2000; 407: 364–367. PMID: 11014189
4. Yoshimura T, Suzuki K, Kiyosawa H, Ono T, Hattori H, Kuma K, et al. Impacts of elevated CO_2 on particulate and dissolved organic matter production: microcosm experiments using iron-deficient plankton communities in open subarctic waters. J Oceanogr. 2013; 69: 601–618.
5. Yoshimura T, Sugie K, Endo H, Suzuki K, Nishioka J, Ono T. Organic matter production response to CO_2 increase in open subarctic plankton communities: Comparison of six microcosm experiments under iron-limited and-enriched bloom conditions. Deep Sea Res I. 2014; 94: 1–14.

6. Hutchins DA, Fu FX, Zhang Y, Warner ME, Feng Y, Portune K, et al. CO_2 control of Trichodesmium N_2 fixation, photosynthesis, growth rates, and elemental ratios: implications for past, present, and future ocean biogeochemistry. Limnol Oceanogr. 2007; 52: 1293–1304.
7. Sun J, Hutchins DA, Feng Y, Seubert EL, Caron DA, Fu FX. Effects of changing pCO_2 and phosphate availability on domoic acid production and physiology of the marine harmful bloom diatom *Pseudo-nitzschia multiseries*. Limnol Oceanogr. 2011; 56: 829–840.
8. Sugie K, Yoshimura T. Effects of pCO_2 and iron on the elemental composition and cell geometry of the marine diatom *Pseudo-nitzschia pseudodelicatissima* (Bacillariophyceae). J Phycol. 2013; 49: 475–488. doi: 10.1111/jpy.12054 PMID: 27007037
9. Nelson DM, Tréguer P, Brzezinski MA, Leynaert A, Quéguiner B. Production and dissolution of biogenic silica in the ocean: Revised global estimates, comparison with regional data and relationship to biogenic sedimentation. Global Biogeochem Cy. 1995; 9: 359–372.
10. Riebesell U, Tortell PD. Effects of ocean acidification on pelagic organisms and ecosystems. In: Gattuso JP, Hansson L, editors. Ocean acidification. Oxford University Press, New York; 2011. p. 99–121.
11. Kroeker KJ, Kordas RL, Crim R, Hendriks IE, Ramajo L, Singh GS, et al. Impacts of ocean acidification on marine organisms: quantifying sensitivities and interaction with warming. Glob Change Biol. 2013; 19(6): 1884–1896.
12. Tortell PD, DiTullio GR, Sigman DM, Morel FM. CO_2 effects on taxonomic composition and nutrient utilization in an Equatorial Pacific Phytoplankton assemblage. Mar Ecol Prog Ser. 2002; 236: 37–43.
13. Feng YY, Hare CE, Leblance K, Rose JM, Zhang YH, DiTullio GR, et al. Effects of increased pCO_2 and temperature on the North Atrantic spring bloom. I. The phytoplankton community and biogeochemical response. Mar Ecol Prog Ser. 2009; 388: 13–25.
14. Hoppe CJ, Hassler CS, Payne CD, Tortell PD, Rost B, Trimborn S. Iron limitation modulates ocean acidification effects on Southern Ocean phytoplankton communities. PloS One. 2013; 8: e79890. doi: 10.1371/journal.pone.0079890 PMID: 24278207
15. Engel A, Schulz KG, Riebesell U, Bellerby R, Delille B, Schartau M. Effects of CO_2 on particle size distribution and phytoplankton abundance during a mesocosm bloom experiment (PeECE II). Biogeosciences. 2008; 5: 509–521.
16. Endo H, Yoshimura T, Kataoka T, Suzuki K. Effects of CO_2 and iron availability on phytoplankton and eubacterial community compositions in the northwest subarctic Pacific. J Exp Mar Biol Ecol. 2013; 439: 160–175.
17. Hare CN, Leblanc K, DiTullio GR, Kudela RM, Zhang Y, Lee PA, et al. Consequences of increased temperature and CO_2 for phytoplankton community structure in the Bering Sea. Mar Ecol Prog Ser. 2007; 352: 9–16.
18. Sugie K, Endo H, Suzuki K, Nishioka J, Kiyosawa H, Yoshimura T. Synergistic effects of pCO_2 and iron availability on nutrient consumption ratio of the Bering Sea phytoplankton community. Biogeosciences. 2013; 10: 6309–6321.
19. Yang G, Gao K. Physiological responses of the marine diatom *Thalassiosira pseudonana* to increased pCO_2 and seawater acidity. Mar Env Res. 2012; 79: 142–151.
20. Midorikawa T, Iwano S, Saito K, Takano H, Kamiya H, Ishii M, et al. Seasonal changes in oceanic pCO_2 in the Oyashio region from winter to spring. J Oceanogr. 2003; 59: 871–882.
21. Fielding AS, Turpin DH, Guy RD, Calvert SE, Crawford DW, Harrison PJ. Influence of the carbon concentrating mechanism on carbon stable isotope discrimination by the marine diatom *Thalassiosira pseudonana*. Can J Bot. 1998; 76: 1098–1103.
22. Trimborn S, Wolf-Gladrow D, Richter KU, Rost B. The effect of pCO_2 on carbon acquisition and intracellular assimilation in four marine diatoms. J Exp Mar Biol Ecol. 2009; 376: 26–36.
23. Tortell PD, Payne CD, Li Y, Trimborn S, Rost B, Smith WO, et al. CO_2 sensitivity of Southern Ocean phytoplankton. Geophys Res Lett. 2008; 35.
24. Bhadury P, Ward BB. Molecular diversity of marine phytoplankton communities based on key functional genes. J Phycol. 2009; 45: 1335–1347. doi: 10.1111/j.1529-8817.2009.00766.x PMID: 27032591
25. Tai V, Palenik B. Temporal variation of *Synechococcus* clades at a coastal Pacific Ocean monitoring site. ISME. J. 2009; 3: 903–915. doi: 10.1038/ismej.2009.35 PMID: 19360028
26. Kirkham AR, Lepère C, Jardillier LE, Not F, Bouman H, Mead A, et al. A global perspective on marine photosynthetic picoeukaryote community structure. ISME J. 2013; 7: 922–936 doi: 10.1038/ismej.2012.166 PMID: 23364354
27. Endo H, Sugie K, Yoshimura T, Suzuki K. Effects of CO_2 and iron availability on *rbcL* gene expression in Bering Sea diatoms. Biogeosciences. 2015; 12: 2247–2259.

28. Hopkinson BM, Xu Y, Shi D, McGinn PJ, Morel FM. The effect of CO_2 on the photosynthetic physiology of phytoplankton in the Gulf of Alaska. Limnol Oceanogr. 2010; 55: 2011–2024.
29. Meakin NG, Wyman M. Rapid shifts in picoeukaryote community structure in response to ocean acidification. ISME J. 2011; 5: 1397–1405. doi: 10.1038/ismej.2011.18 PMID: 21412344
30. Newbold LK, Oliver AE, Booth T, Tiwari B, DeSantis T, Maguire M, et al. The response of marine picoplankton to ocean acidification. Environ Microbiol. 2012; 14: 2293–2307. doi: 10.1111/j.1462-2920.2012.02762.x PMID: 22591022
31. Corredor JE, Wawrik B, Paul JH, Tran H, Kerkhof L, Lopez JM, et al. Geochemical rate-RNA integrated study: ribulose-1,5-bisphosphate carboxylase/oxygenase gene transcription and photosynthetic capacity of planktonic photoautotrophs. Appl Environ Microbiol. 2004; 70: 5459–5468. PMID: 15345433
32. John DE, Wang ZA, Liu XW, Byrne RH, Corredor JE, Lopez JM, et al. Phytoplankton carbon fixation gene (RuBisCO) transcripts and air-sea CO_2 flux in the Mississippi River plume. ISME J. 2007; 1: 517–531. PMID: 18043653
33. Granum E, Roberts K, Raven JA, Leegood RC. Primary carbon and nitrogen metabolic gene expression in the diatom *Thalassiosira pseudonana* (Bacillariophyceae): Diel periodicity and effects of inorganic carbon and nitrogen. J Phycol. 2009; 45: 083–1092.
34. John DE, López-Díaz JM, Cabrera A, Santiago NA, Corredor JE, Bronk DA, et al. A day in the life in the dynamic marine environment: how nutrients shape diel patterns of phytoplankton photosynthesis and carbon fixation gene expression in the Mississippi and Orinoco River plumes. Hydrobiologia. 2012; 679: 155–173.
35. Li G, Campbell DA. Rising CO_2 interacts with growth light and growth rate to alter photosystem II photoinactivation of the coastal diatom *Thalassiosira pseudonana*. PLoS One. 2013; 8(1): e55562. doi: 10.1371/journal.pone.0055562 PMID: 23383226
36. Sanger F, Nicklen S, Coulson AR. DNA sequencing with chain-terminating inhibitors. Proc Natl Acad Sci USA. 1977; 74: 5463–5467. PMID: 271968
37. Bent SJ, Forney LJ. The tragedy of the uncommon: understanding limitations in the analysis of microbial diversity. ISME J. 2008; 2: 689–695. doi: 10.1038/ismej.2008.44 PMID: 18463690
38. Shokralla S, Spall JL, Gibson JF, Hajibabaei M. Next-generation sequencing technologies for environmental DNA research. Mol Ecol. 2012; 21: 1794–1805. doi: 10.1111/j.1365-294X.2012.05538.x PMID: 22486820
39. Liu L, Li Y, Li S, Hu N, He Y, Pong R, et al. Comparison of next-generation sequencing systems. J Biomed Biotechnol. 2012. doi: 10.1155/2012/251364
40. Jing H, Xia X, Suzuki K, Liu H. Vertical profiles of bacteria in the tropical and subarctic oceans revealed by pyrosequencing. PloS One. 2013; 8: e79423. doi: 10.1371/journal.pone.0079423 PMID: 24236132
41. Bittner L, Gobet A, Audic S, Romac S, Egge ES, Santini S, et al. Diversity patterns of uncultured Haptophytes unravelled by pyrosequencing in Naples Bay. Mol Ecol. 2013; 22: 87–101. doi: 10.1111/mec.12108 PMID: 23163508
42. Hirai J, Kuriyama M, Ichikawa T, Hidaka K, Tsuda A. A metagenetic approach for revealing community structure of marine planktonic copepods. Mol Ecol Resour. 2015; 15: 68–80. doi: 10.1111/1755-0998.12294 PMID: 24943089
43. Takahashi T, Sutherland SC, Sweeney C, Poisson A, Metzl N, Tibrook B, et al. Global sea-air CO_2 flux based on climatological surface ocean pCO_2, and seasonal biological and temperature effects. Deep-Sea Res II. 2002; 49: 1601–1622.
44. Liu H, Suzuki K, Saito H. Community structure and dynamics of phytoplankton in the western subarctic Pacific Ocean: A synthesis. J Oceanogr. 2004; 60: 119–137.
45. Hattori-Saito A, Nishioka J, Ono T, McKay RML, Suzuki K. Iron deficiency in micro-sized diatoms in the Oyashio region of the western subarctic Pacific during spring. J Oceanogr. 2010; 66: 105–115.
46. Sugie K, Kuma K, Fujita S, Ikeda T. Increase in Si:N drawdown ratio due to resting spore formation by spring bloom-forming diatoms under Fe-and N-limited conditions in the Oyashio region. J Exp Mar Biol Ecol. 2010; 382: 108–116.
47. Suzuki K, Kuwata A, Yoshie N, Shibata A, Kawanobe K, Saito H. Population dynamics of phytoplankton, heterotrophic bacteria, and viruses during the spring bloom in the western subarctic Pacific. Deep-Sea Res I. 2011; 58: 575–589.
48. Taniguchi A. Differences in the structure of the lower trophic levels of pelagic ecosystems in the eastern and western subarctic Pacific. Progr Oceanogr. 1999; 43: 289–315.
49. Sakurai Y. An overview of the Oyashio ecosystem. Deep-Sea Res II. 2007; 54: 2526–2542.

50. Edmond JM. High precision determination of titration alkalinity and total carbon dioxide content of sea water by potentiometric titration. Deep-Sea Res. 1970; 17: 737–750.

51. Lewis E, Wallace D, Allison LJ. Program developed for CO_2 system calculations. Tennessee. Carbon Dioxide Information Analysis Center, managed by Lockheed Martin Energy Research Corporation for the US Department of Energy. 1998.

52. Suzuki R, Ishimaru T. An improved method for the determination of phytoplankton chlorophyll using N, N-dimethylformamide. J Oceanogr. Soc. Japan. 1990; 46: 190–194.

53. Welschmeyer NA. Fluorometric analysis of chlorophyll a in the presence of chlorophyll *b* and pheopigments. Limnol Oceanogr. 1994; 39: 1985–1992.

54. Mackey MD, Mackey DJ, Higgins HW, Wright SW. CHEMTAX-a program for estimating class abundances from chemical markers: application to HPLC measurements of phytoplankton. Mar Ecol Prog Ser. 1996; 144: 265–283.

55. John DE, Patterson SS, Paul JH. Phytoplankton group specific quantitative polymerase chain reaction assays for RuBisCO mRNA transcripts in seawater. Mar. Biotechnol. 2007; 9: 747–759. PMID: 17694413

56. Schloss PD, Westcott SL, Ryabin T, Hall JR, Hartmann M, Hollister EB, et al. Introducing mothur: open-source, platform-independent, community-supported software for describing and comparing microbial communities. Appl Environ Microb. 2009; 75: 7537–7541.

57. Shannon CE. A mathematical theory of communication. AT&T Teck J. 1948; 27: 379–423.

58. Simpson EH. Measurement of diversity. Nature. 1949; 163: 688.

59. Gieskes WWC, Kraay GW. Dominance of Cryptophyceae during the phytoplankton spring bloom in the central North Sea detected by HPLC analysis of pigments. Mar Biol. 1983; 75: 179–185.

60. Isada T, Kuwata A, Saito H, Ono T, Ishii M, Yoshikawa-Inoue H, et al. Photosynthetic features and primary productivity of phytoplankton in the Oyashio and Kuroshio–Oyashio transition regions of the northwest Pacific. Journal of Plankton Res. 2009; 31: 1009–1025.

61. Yoshie N, Suzuki K, Kuwata A, Nishioka J, Saito H. Temporal and spatial variations in photosynthetic physiology of diatoms during the spring bloom in the western subarctic Pacific. Mar Ecol Prog Ser. 2010; 399: 39–52.

62. Wu Y, Campbell DA, Irwin AJ, Suggett DJ, Finkel ZV. Ocean acidification enhances the growth rate of larger diatoms. Limnol Oceanogr. 2014; 59(3): 1027–1034.

63. Gao K, Xu J, Gao G, Li Y, Hutchins DA, Huang B, et al. Rising CO_2 and increased light exposure synergistically reduce marine primary productivity. Nature Clim Change. 2012; 2: 519–523.

64. Rose JM, Feng Y, Gobler CJ, Gutierrez R, Hare CE, Leblanc K, et al. Effects of increased pCO_2 and temperature on the North Atlantic spring bloom. II. Microzooplankton abundance and grazing. Mar Ecol Prog Ser. 2009; 388: 27–40.

65. Losh JL, Young JN, Morel FM. Rubisco is a small fraction of total protein in marine phytoplankton. New Phytol. 2013; 198: 52–58. doi: 10.1111/nph.12143 PMID: 23343368

66. Losh JL, Morel FM, Hopkinson BM. Modest increase in the C: N ratio of N-limited phytoplankton in the California Current in response to high CO_2. Mar Ecol Prog Ser. 2012; 468: 31–42.

67. Venrick EL, Beers JR, Heinbokel JF. Possible consequences of containing microplankton for physiological rate measurements. J Exp Mar Biol Ecol. 1977; 26: 55–76.

68. Nogueira P, Domingues RB, Barbosa AB. Are microcosm volume and sample pre-filtration relevant to evaluate phytoplankton growth? J Exp Mar Biol Ecol. 2014; 461: 323–330.

69. Schulz KG, Riebesell U, Bellerby RGJ, Biswas H, Meyerhöfer M, Müller MN, et al. Build-up and decline of organic matter during PeECE III. Biogeosciences. 2008; 5: 707–718.

70. Burkhardt S, Amoroso G, Riebesell U, Sültemeyer D. (2001). CO_2 and HCO3– uptake in marine diatoms acclimated to different CO_2 concentrations. Limnol Oceanogr. 2001; 46; 1378–1391.

71. Rost B, Riebesell U, Burkhardt S, Sültemeyer D. Carbon acquisition of bloom forming marine phytoplankton, Limnol Oceanogr. 2003; 48: 55–67.

72. Trimborn S, Lundholm N, Thoms S, Richter KU, Krock B, Hansen PJ, et al. Inorganic carbon acquisition in potentially toxic and non-toxic diatoms: the effect of pH-induced changes in seawater carbonate chemistry. Physiologia Plantarum. 2008; 133: 92–105. doi: 10.1111/j.1399-3054.2007.01038.x PMID: 18405335

73. Raven JA. Inorganic carbon acquisition by eukaryotic algae: four current questions. Photosynth Res. 2010; 106: 123–134. doi: 10.1007/s11120-010-9563-7 PMID: 20524069

74. Chiba S, Ono T, Tadokoro K, Midorikawa T, Saino T. Increased stratification and decreased lower trophic level productivity in the Oyashio region of the North Pacific: A 30-year retrospective study. J Oceanogr. 2004; 60: 149–162.

75. Chiba S, Batten S, Sasaoka K, Sasai Y, Sugisaki H. Influence of the Pacific Decadal Oscillation on phytoplankton phenology and community structure in the western North Pacific. Geophys Res Lett. 2012; 39.15. doi: 10.1029/2012GL052912